Available online at www.sciencedirect.com

ScienceDirect

journal homepage: http://www.elsevier.com/locate/aob

Novel *missense* mutation of the *FAM83H* gene causes retention of amelogenin and a mild clinical phenotype of hypocalcified enamel

Blanca Urzúa [a,e,*], *Carolina Martínez* [a,e], *Ana Ortega-Pinto* [b], *Daniela Adorno* [b], *Irene Morales-Bozo* [a], *Gonzalo Riadi* [c], *Lilian Jara* [d], *Anita Plaza* [a], *Claudia Lefimil* [a], *Carla Lozano* [a], *Monserrat Reyes* [b]

[a] *Institute for Research in Dental Sciences, Faculty of Dentistry, University of Chile, Sergio Livingstone Ave. N° 943, Independencia, Santiago, Chile*

[b] *Department of Pathology and Oral Medicine, Faculty of Dentistry, University of Chile, Sergio Livingstone Ave. N° 943, Independencia, Santiago, Chile*

[c] *Center of Bioinformatics and Molecular Simulations, CBSM, Faculty of Engineering, University of Talca, 2 norte Ave. N° 685, Talca, Chile*

[d] *Institute of Biomedical Sciences, Faculty of Medicine, University of Chile, Independencia Ave. N° 1027, Santiago, Chile*

ARTICLE INFO

Article history:
Received 27 February 2015
Received in revised form
10 June 2015
Accepted 11 June 2015

Keywords:
Amelogenesis
Missense mutation
FAM83H gene
Amelogenin retention
Mild phenotype

ABSTRACT

Objective: Amelogenesis imperfecta (AI) is a group of clinically and genetically heterogeneous inherited conditions, causing alterations in the structure of enamel and chemical composition of enamel matrix during development. The objective of this study was to compare the clinical, radiographic, histological and immunohistochemical phenotypes of subjects affected with hypocalcified AI from three Chilean families and identify causal mutations in the *FAM83H* gene.

Design: The diagnosis was made using clinical, radiographic, histological and genealogical data from the patients, who were evaluated according to the classification criteria by Witkop. PCR and Sanger sequencing of the complete coding sequence and surrounding intron regions of the *FAM83H* gene were conducted. The structural study of the affected teeth was performed with light microscopy, scanning electron microscopy and immunohistochemistry.

Results: The probands of the three families were diagnosed with hypocalcified AI, but in only one of them the *missense* variant p.Gly557Cys was identified. This variant was not present in the SNP database or in 100 healthy controls and segregated with the disease in the affected family. Using light microscopy, a normal prismatic structure was observed in all three cases. However, the ultrastructure was found to be affected in two of the cases, showing persistence of organic matter including amelogenins.

* *Corresponding author*. Tel.: +56 2 29781793, +56 9 99134895.
E-mail addresses: brurzua@gmail.com (B. Urzúa), carolina_aml@yahoo.com (C. Martínez), aveortega@gmail.com (A. Ortega-Pinto), daniadorno@gmail.com (D. Adorno), irenemoralesbozo@gmail.com (I. Morales-Bozo), griadi@gmail.com (G. Riadi), ljara@med.uchile.cl (L. Jara), anitaplazaflores@yahoo.com (A. Plaza), claulefi@gmail.com (C. Lefimil), carlalozan@gmail.com (C. Lozano), montserrat.reyes.r@gmail.com (M. Reyes).
[e] Equal authorship.

http://dx.doi.org/10.1016/j.archoralbio.2015.06.016

Conclusions: These results suggest that *FAM83H missense* mutation reported in one of the families analyzed in this study might cause a phenotype of hypocalcified enamel more attenuated with retention of amelogenin.

1. Introduction

The process of forming the enamel (amelogenesis) occurs in two stages: the secretion of an organic matrix and the subsequent mineralization of that matrix. During the secretory stage, ameloblasts deposit a matrix layer rich in protein, partially mineralized, over the previously formed dentine until reaching the complete thickness of the future enamel. These proteins are 90% amelogenins, while the remaining 10% contains ameloblastin, enamelin, tuftelin, enamelysin, kallikrein and other proteins. During the maturation stage, the removal of organic materials and water and the continuous deposition of phosphate and calcium convert enamel into the hardest tissue in the human body.[1–3]

The normal process of amelogenesis is regulated by the expression of multiple genes. Mutations in any of these genes may result in changes in tissue formation, consequently alter enamel phenotypes. Defective synthesis of enamel is called amelogenesis imperfecta (AI). AI is defined as a group of genetic disorders that affect, to varying degrees, the structure and appearance of the enamel of all or nearly all the teeth in either the primary or permanent dentition or both[4,5] and may occur as an isolated condition that only affects the enamel or in association with abnormalities in other tissues.[6,7]

AI has been classified into three main types, whose defects are correlated with the stages of enamel formation. In hypoplastic AI, the enamel is thin or contains defects due to inadequate apposition in localized or generalized areas, but has a higher radiopacity than dentine. In hypocalcified AI, the enamel is of normal thickness, but there is a defect in the nucleation and mineralization of the prisms, which results in soft enamel that is easily removable and less radiopaque than dentine. In hypomature AI, although the enamel thickness is normal, there is a defect in protein removal and the growth of crystals during the maturation stage, resulting in enamel with abnormal hardness and transparency and a decreased radiopacity similar to that of dentine.[8–10]

The AI prevalence varies widely depending on the population studied; for example, the reported figures are 1:4000 in Sweden,[11] 1:8000 in Israeli Jews[12] and 1:14,000 in the U.S.[13] For Chile, there are no data on the prevalence and/or incidence of AI.

To date, mutations in genes encoding secreted proteins of the enamel matrix (e.g., *AMELX*, *ENAM* and *AMBN*), enamel proteases (e.g., *MMP20* and *KLK4*) and proteins that participate in biomineralization (e.g., *C4orf26*), ion transport (e.g., *SLC24A4* and *STIM1*) and the cytoskeletal organization of keratins (e.g., *FAM83H*), intracellular vesicular traffic (e.g., *WDR72*) and cellular adhesion proteins (e.g., *LAMB3* and *ITGB6*) have been shown to cause non-syndromic AI, with various patterns of inheritance. Eighteen mutations in different positions on the *AMELX* gene are responsible for cases of hypoplastic or hypoplastic/hypomaturation AI with patterns of X-linked inheritance.[14–16] The molecular defects underlying the various clinical forms of autosomal dominant hypoplastic AI (ADAI) are ten and five mutations in the *ENAM* and *LAMB3* genes, respectively.[10,17–20] Moreover, two mutations in the *ENAM* gene,[21,22] 5 mutations in the *C4orf26* gene[23] and 4 mutations in the *ITGB6* gene were recently reported to cause hypoplastic AI with an autosomal recessive pattern of inheritance (ARAI).[24,25] Mostly recently, a deletion of ameloblastin exon 6 (*AMBN*) has been associated with hypoplastic ARAI.[26]

The ARAI form of hypomature type can be caused by seven mutations in the enamelysin (*MMP-20*) gene,[10,27,28] two mutations in the kallikrein 4 gene (*KLK4*),[27,29] six mutations in the *WDR72* gene,[9,10,30] four mutations in the *SLC24A4* gene[31,32] and one mutation in the *STIM1* gene.[33] The autosomal dominant forms of hypocalcified AI are associated with 20 defects in exon 5 of the *FAM83H* gene.[7,10,34–44]

In this paper, we report the results of a clinical and molecular genetic study of three Chilean families with hypocalcified AI, focusing our efforts on the analysis of the complete coding sequence and exon–intron junctions of the *FAM83H* gene, the most likely candidate for autosomal dominant hipocalcified AI (ADHCAI).

2. Materials and methods

2.1. Study subjects

Three unrelated Chilean families, including three probands affected with hypocalcified AI (two men and a woman) and eight healthy individuals (five women and three men), who are parents and siblings of the probands, participated in this study. The features and objectives of the research were explained to the eleven participants, who voluntarily signed a written informed consent form. This research was approved by the Ethical Scientific Committee (Act No.: 2013/06) and the Institutional Biosafety Committee of the Faculty of Dentistry (FDO No.: 2, June 24, 2013), University of Chile, and was conducted in full accordance with the ethical principles of the Declaration of Helsinki[45] and local regulations.

2.2. Diagnosis of AI

The extra and intraoral clinical examination was conducted at the Diagnostic Service of Faculty of Dentistry, University of Chile, and was executed by two trained dental surgeons (AOP and DAF), who reached a consensus diagnosis. The participants were asked about systemic diseases, treatment with tetracycline, fluoride consumption and any other information that may affect the structure of their teeth during development.

The examination was performed with a No. 5 mirror and caries probe while air-drying the teeth being examined. Data were collected on anterior open bite, enamel hardness, changes in the shape and colour of teeth, such as the loss of contact points and alterations of the enamel surface, enamel wear and detachment from the underlying dentine. The affected and unaffected individuals were also clinically evaluated for the presence of abnormalities of the skin, hair, nails and bones, known to be a sign of syndromic conditions associated with AI. The clinical diagnosis were made based on historical, clinical, radiographic and genealogical data of the patients, who were evaluated according to the criteria of classification by Witkop.[4] The following features were clinically evaluated in the affected individuals to determine whether a patient had hypocalcified AI: (1) soft, brittle enamel that is rapidly lost, revealing dentine, except in cervical areas and cusp tips, (2) tooth crowns having a cheesy or clay appearance often accumulate large deposits of calculus and their enamel radiographically less radiopaque than dentine, (3) enamel of unerupted or recently erupted teeth has a normal thickness, as determined by either radiography or clinical examination, (4) presence of a radiodense line of calcified enamel remaining in the cervical area and (5) yellowish-brown enamel that becomes brown or black due to extrinsic pigmentation acquired after the eruption.

2.3. Radiographic analysis

Periapical radiographs were taken (Heliodent DS, Siemens, Germany) of all affected individuals to detect the radiopacity of enamel and dentine, contrast between enamel and dentine, enamel thickness and to evaluate taurodontism. Additionally, left lateral cephalometric films were obtained (Orthophos DS, Siemens, Germany) from all affected participants in each family, and a cephalometric analysis with Björk-Jarabak and Steiner's SNA and SNB traces (Quick Ceph 2.0) were conducted to assess skeletal open bite.

2.4. Molecular genetic analysis

Pedigree was constructed base on the family history of AI disease using interviews of the probands, their parents and relatives who provided informed consent to participate. For DNA purification, 10 ml of venous blood was taken from the patients and control subjects, and the genomic DNA was isolated from leukocytes by the salting-out method described by Miller et al.[46] Complete sequencing of the coding regions and surrounding introns of the *FAM83H* gene in the probands of the three families was performed by amplification via polymerase chain reaction (PCR) with oligonucleotide primers designed based on the reference sequence of the *FAM83H* gene (NG_016652.1) using the Primer-BLAST software.[47] The sequence and size of each amplified product and the associated annealing temperature are described in Table 1. The PCR products were extracted from agarose gels and purified using the Ultraclean® 15 DNA purification kit from Mo Bio Laboratories, Inc. (CA 92010, United States). The purified amplicons were sequenced in both directions by the DNA sequencing centre in Macrogen, Seoul, Korea. For computational sequence analysis, Vector NTI version 10.0 software and *FAM83H* gene reference sequences NG_016652.1 and NM_198488.3 were used. The detection of variant g.10953G>T in control subjects was conducted by direct sequencing and by Restriction Fragment Length Polymorphism-coupled PCR (RFLP-PCR), using primers that amplify a 332-bp fragment of exon 5 of the FAM83H gene (Table 1) and digestion with the *ApaI* restriction enzyme.

2.5. Histological analysis

Ground sections. For the histological analysis of AI-affected teeth, three teeth were examined: one deciduous second molar exfoliated physiologically (proband III.5 of the FAI2 family) and two permanent third molars extracted for orthodontic purposes (probands II.1 of the FAI5 and FAI14 families, respectively). Additionally, two teeth donated voluntarily by healthy individuals not related with the families were used as controls (deciduous molar and third molar). These teeth were subjected to wear with a diamond-cutting saw and were mounted for examination by light microscopy.

Scanning electron microscopy (SEM). The teeth were cleaned with 5% sodium hypochlorite, fractured and dehydrated in ascending acetone concentrations of 70%, 90% and 100%. The metallic finish and drying were performed at the Laboratory of Scanning Electron Microscopy in a Zeiss microscope model DMS 940 from the Faculty of Medicine, University of Chile.

Immunohistochemistry. For antigen retrieval, the cuts were exposed to 0.01 M citrate buffer (pH 6) in a heat source at 95 °C for 20 min. To block endogenous peroxidase activity, the sections were placed in 3% hydrogen peroxide in methanol for 10 min at room temperature. Sections of 5 μm were incubated with anti-human-amelogenin (Anti-AMELX produced in rabbit, polyclonal, diluted 1:200; Sigma HPA-005988, Sigma–Aldrich®) and Amelogenin code F-11 produced in mouse, monoclonal, diluted 1:2500; sc-365284 code, Santa Cruz Biotechnology®) for 20 min at room temperature. Subsequently, the cuts were washed in PBS and incubated with the biotinylated secondary antibody for 20 min at 37 °C. The avidin–biotin–peroxidase complex was used to bind the primary antibody using VECTASTAIN® (ABC, CA 94010, United States). The reaction products were visualized by immersion of the histopathological sections in diaminobenzidine (DAB) in the case of anti-AMELX and aminoethylcarbazole (AEC) for amelogenin antibody F-11 for 3–5 min. Nuclear counterstaining was performed with Harris haematoxylin. To study the negative controls for the antibodies, sections were treated with phosphate-buffered saline instead of primary antibody, and the absence of staining was confirmed. The positive controls used tooth germ in the advanced bell stage from a tumour resection and an included third permanent molar obtained from a dentigerous cyst.

2.6. Bioinformatic analysis

The effect of the sequence variant found in the *FAM83H* gene of the proband in the family FAI14 was predicted using the computer programmes Polymorphism Phenotyping v2 (PolyPhen),[48] Protein ANnotation THrough Evolutionary Relationship (PANTHER)[49] and Pathological Mutations (PMut).[50] The analysis of the pattern of disulfide bonds was performed with the server DiAminoacid Neural Network Application (DiANNA),[51] and the analysis of the interactions with other

Table 1 – Primers designed with the Primer-BLAST programme to amplify and sequence the *FAM83H* gene in probands and controls of the study.

Exon	Primer name	Sequence 5′ → 3′	PCR product size (pb)	Annealing temperature (°C)
1	FAMex1F	GGTCAGGGGTCAGGCTGGGAACT	744	65
	FAMex1R	CACCCAGACTCCAGCTAGGCCG		
2	FAMex2aF	AGGGGCATCCTAGGGTCTGG	921	64
	FAMex2aR	AATGAACCCAGGCTGGTGGG		
3 y 4	FAMex3-4aF	GAATGGGGGCAGCTCAGC	900	62
	FAMex3-4aR	GTCAAACCGAGCTGGAGCGA		
	FAMex3-4bF	GGGTGTGGAGGGGAGGCTGG	503	62
	FAMex3-4bR	GTGGAAAGGGGGTGCTGGGG		
5	FAMex5aF	CTGTAACCCCAGCACCCCCTTTC	932	64
	FAMex5aR	GGTGAAGTCATCCGGGTCCGC		
	FAMex5b1F	CCTTCAAGCGGCACAGCTTC	931	64
	FAMex5b1R	CTGACCGTCTGCTCCTTGTG		
	FAMex5b2F	CAGTGGGACCCGCAGCTCAC	642	63
	FAMex5b2R	CAGGCGCGAGCGGAATGAGT		
	FAMex5c1F	GGAGGCTTACGAAGACGACG	913	66
	FAMex5c1R	CTCGGGGTAGGCTGAGGTG		
	FAMex5c2F	AGCAGGACTCATTCCGCTCG	626	66
	FAMex5c2R	GGTGGGGCTCCCTTTTGACT		
	FAMex5d1F	CTTCCTCTCTGCCCAGAGCC	900	62
	FAMex5d1R	CTGTACACGCGCTTCTCCTT		
	FAMex5d2F	CACCTCGGCTTACCCTGAGC	602	62
	FAMex5d2R	CTAGCTCGGGGCTGTTGTGG		
	FAMex5e1F	CGAAGGCCATTCTGGAGCAG	1075	62
	FAMex5e1R	GGAATTGAGGCACAGAGGCG		
	FAMex5e2F	CACAACAGCCCCGAGCTAGG	621	62
	FAMex5e2R	CAAGGCTGACGGTGCAGAGA		
	FAMex5f1F	GCAGCGTCTGGCTCCG	902	63
	FAMex5f1R	ACTCCACAACCAGCCCTTCT		
	FAMex5f2F	ATCCTCTTGCAAGGGTCTCG	451	63
	FAMex5f2R	CCCTCCCCACTCTCACCC		
	FAMex5g1F	TGGACCAGAAGATGCCCCTT	948	64
	FAMex5g1R	TCTCCATGGACTCCAGCTGG		
	FAMex5g2F	TTTGCAGCACAGTAAAACATGGTCC	600	64
	FAMex5g2R	GGCTGTGCAGGAGTGAAAGTG		
	FAMex5hF	ACCACGTGTGTAGAAAGCCCCCAC	600	63
	FAMex5hR	GGGGAAATCTGGGAGGCCACGT		
	Ex5b332F	CGCTTCCCGGAGCTCGGACCC	332	72
	Ex5b332R	CGCTTCCCGGAGCTCGGACCC		

proteins used the Database of Interacting Proteins (DIP)[52] and Human Protein–Protein Interaction Prediction (PIPs).[53] Sequence information for the variants was submitted to a SNP database (dbSNP)[54] and was assigned the identification numbers of ss715578273 and rs312262803.

3. Results

3.1. *Clinical and radiographic findings*

In this study, three unrelated Chilean families were diagnosed with hypocalcified AI. The clinical, radiographic and cephalometric parameters of two of the probands (FAI2, subject III.5 and FAI5, subject II.1) were described in detail in a previous study.[55] As seen in the clinical picture presented in Fig. 1A, the teeth of the proband III.5 of family FAI2 have a yellowish-brown colouration and rough surface. This enamel was soft, which was evident by the wear of cusps and incisal edges and enamel largely missing from the crown, except in the cervical region, which was relatively better preserved (Fig. 1A, clinical picture, black arrowheads). The patient had dental hypersensitivity to heat stimuli, generalized gingivitis and multiple composite resins restorations, some of which were fractured (Fig. 1A, clinical picture, white arrowhead). The proband also had delayed eruption, and cephalometrically, he presented balanced mesomorphic facial profile. Radiographically, there was a similar contrast between enamel and dentine and generalized detachment of the enamel from the erupted teeth, similar to adits were observed (Fig. 1A, upper radiography, white arrowheads); in contrast, those teeth that had not erupted exhibited normal crown anatomy, with enamel of normal thickness but lacking contrast from the dentine (Fig. 1A, lower radiograph, white arrowhead). The intraoral examination of the parents and two brothers noted no deviation from normal enamel with respect to colour, surface, hardness or thickness.

Similar to the previous case, proband II.1 of family FAI5 had yellowish-brown enamel on all teeth. The enamel had a rough surface and was detached and worn widely, except in the

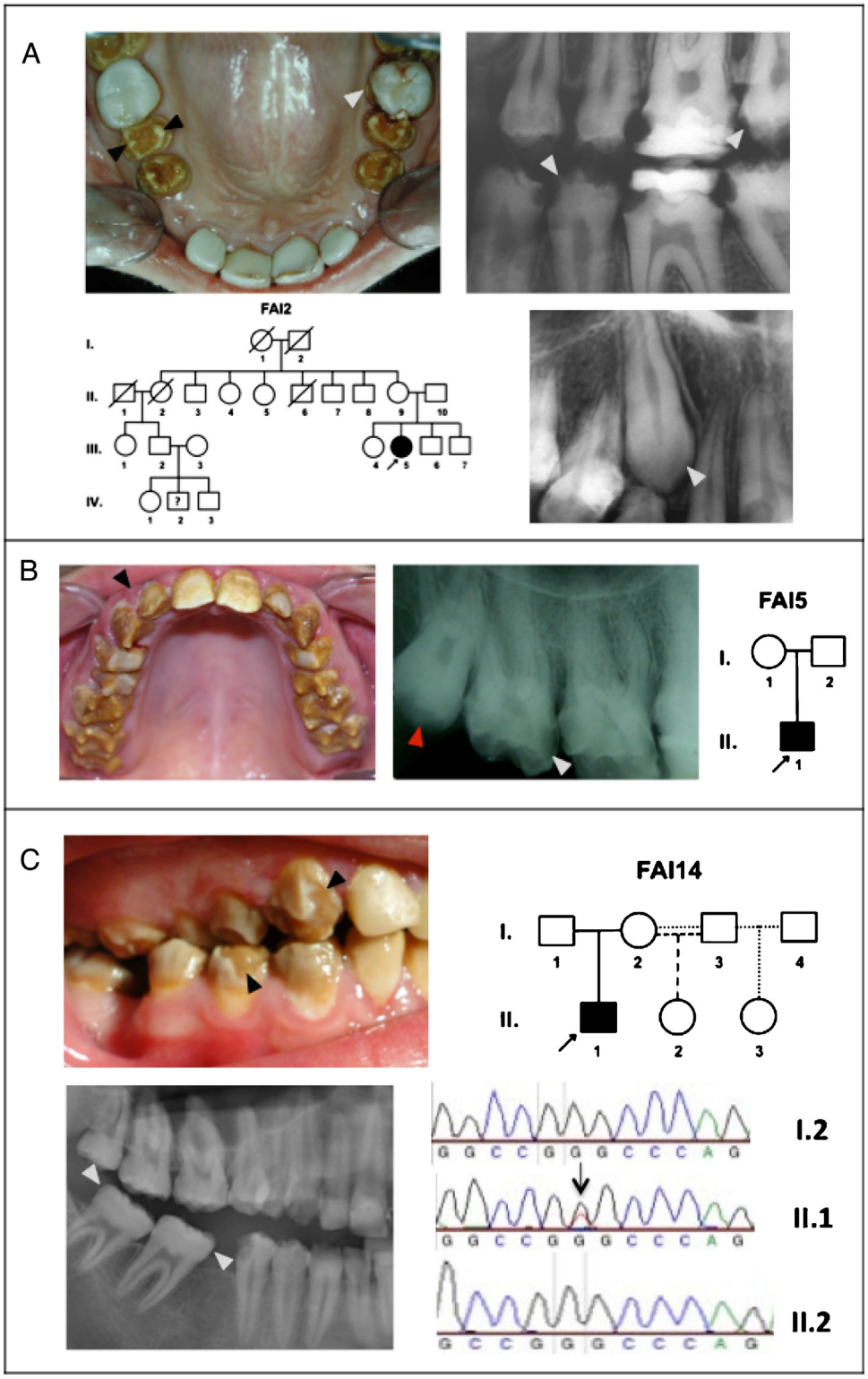

Fig. 1 – Clinical photographs, radiographs, pedigrees and mutational analysis of Chilean families FAI2 (A), FAI5 (B) and FAI14 (C) affected with hypocalcified AI. (For interpretation of the references to colour in text near the reference citation, the reader is referred to the web version of this article.)

cervical region (Fig. 1B, photo clinic). This patient had generalized gingivitis, as noted by the characteristic erythematous interdental papillae and increased volume (Fig. 1B, black arrowhead). This proband also had dental hypersensitivity to thermal stimuli and previous composite restorations, which became detached or fractured shortly after being installed. The radiographic analysis showed that the enamel and dentine were similarly contrasted in both unerupted and

erupted teeth. The erupted teeth had thinner enamel with a tendency of fracture (Fig. 1B, X-ray, white arrowhead), in contrast to the unerupted pieces, which had enamel with an approximately normal thickness on a preserved and fairly normal Crown anatomy (Fig. 1B, X-ray, red arrowhead). The parents of this patient could not be involved, but the patient indicated that they did not present similar abnormalities.

Proband II.1 of family FAI14 had grey-brown enamel with a rough texture, some detached on the labial surfaces (Fig. 1C, clinical picture, black arrowheads) and worn cusps and incisal edges. The enamel in the cervical region maintained an average thickness with a less intense colour. The patient presented tooth hypersensitivity to thermal stimuli, generalized gingivitis and numerous composite restorations in poor condition. Radiographically, in contrast to the previous cases, a somewhat greater contrast in the enamel, especially at the lower molar (Fig. 1C, radiograph, white arrowheads) was observed. These molars, in turn, had near intact clinical crown. The intraoral examination of the mother and two half-sisters did not reveal any alterations in enamel colour, surface hardness or thickness.

3.2. *Molecular genetic analysis*

According to the pedigree shown in Fig. 1A, individual III.5 of family FAI2 was found to be affected, and individual IV.2 was reported to be affected by the mother of the proband, but he was unwilling to be evaluated clinically. In the pedigree shown in Fig. 1B, the parents of the proband were reported to be unaffected. A similar situation was observed in the FAI14 family, whose pedigree (Fig. 1C) shows that the proband is the only affected subject. In this case, we were only able to examine her mother and two half-sisters, who did not have the trait. In addition, the proband's mother reported that neither parent had dental problems. Thus, the data collected from these three families indicate either a recessive inheritance pattern or sporadic cases due to new mutations.

The sequencing analysis of gene *FAM83H* performed in the probands of the three families revealed the presence of a mutation in exon 5 in only one of the probands; subject II.1 of family FAI14 (Fig. 1C, chromatogram of the subject II.1). The other two probands were negative for this analysis. The variant identified corresponds to a transversion substitution that changes a guanine-to-thymine at position 10953 of the genomic DNA (NG_016652.1 reference sequence) and position 1669 of the cDNA (NM_198488.3 reference sequence). A *missense* change occurs at the protein level involving the replacement of a nonpolar amino acid (glycine) by a polar (neutral or uncharged) amino acid (cysteine) at position 557 (NP_940890.3). The co-segregation analysis in the family showed that the mother and older half-sister had no such change in the sequence (Fig. 1C, chromatograms of the subjects I.2 and II.2) and that only the proband carried the variant in a heterozygous state, corroborating that this mutation is dominant. The absence of this variant in the SNP database, the 1000 genomes project database,[56] in 100 healthy control subjects analyzed by PCR-RFLP and 15 controls analyzed by Sanger sequencing was confirmed. Thus, we believe that this variant could correspond to the causal mutation in the family studied.

3.3. *Bioinformatic analysis*

The programme PolyPhen 2.0 predicted that the substitution was most likely pathogenic, with a score of 0.992. The PANTHER programme indicated that the mutation was deleterious with a probability of 0.851, and the PMut programme suggested that the variant was pathological with a probability of 0.841 and a reliability value of 6. These results support the pathogenic role of the mutation found in the proband of the AI14 family.

The mutation reported in this study involves the substitution of glycine at position 557 by a cysteine (p.Gly557Cys). Glycine is an amino acid with a hydrogen side chain, which does not interact with the environment, whereas cysteine, with its sulfhydryl group side chain, can form disulfide bonds with metals. As the wild type FAM83H protein has nine cysteine residues in its amino acid sequence at positions 57, 196, 218, 237, 550, 590, 789, 1090 and 1140, determining whether this substitution may alter the pattern links in the mutated protein compared with the wild-type would be interesting. The prediction analysis performed with the DiANNA programme suggested that the pattern of disulfide bonds in the mutant protein changes. In wild-type FAM83H, C^{590} likely shares a disulfide bond with C^{1090} (score 0.89631). In the mutant protein, C^{557} could establish a disulfide bond with C^{590} (score 0.99824) or C^{1090} (score 0.99436) and is more likely to form a new bond between C^{557} and C^{590}. Moreover, with respect to the formation of bonds with metals, the predictions indicate that only C^{550} might be a possible target for metals and that the remaining cysteines, including the substitution to C^{557}, may not form bonds with metals.

Additionally, the analyses performed with the DIP and PIPS programmes, which predict interactions with other proteins, showed that both the wild-type protein and the mutant had no significant interactions with other proteins.

3.4. *Histological, ultrastructural and immunohistochemical analysis*

Light microscopy analysis with 100X magnification of the cuts by wear observed in those affected with hypocalcified AI; second deciduous molar of proband III.5 from the FAI2 family (Fig. 2A); third molar of proband II.1 from the FAI5 family (Fig. 2B) and third molar of proband II.1 of the FAI14 family (Fig. 2C) revealed no alterations in the structure of the enamel at this level, with the prism structure provided in the three cases being similar to that of the control tooth (Fig. 2D). The SEM analysis enabled the study of the ultrastructure of the teeth of the three affected individuals. In the cases of the second molar of proband III.5 from the FAI2 family (Fig. 2E) and the third molar of proband II.1 from the FAI5 family (Fig. 2F), both teeth had a prismatic structure similar to that of their respective controls (Fig. 2H, third molar). Furthermore, in the third molar of proband II.1 from family FAI14, areas in which the prisms do not maintain a constant thickness, similar to rosary beads, with upraised projections were observed (Fig. 2G), and in other sections of the same piece, a slightly irregular amorphous prismatic structure was observed (not shown).

The histophatological and Immunohistochemical analysis using the anti-amelogenin antibody showed the presence of amelogenin-like proteins through an intense brown staining

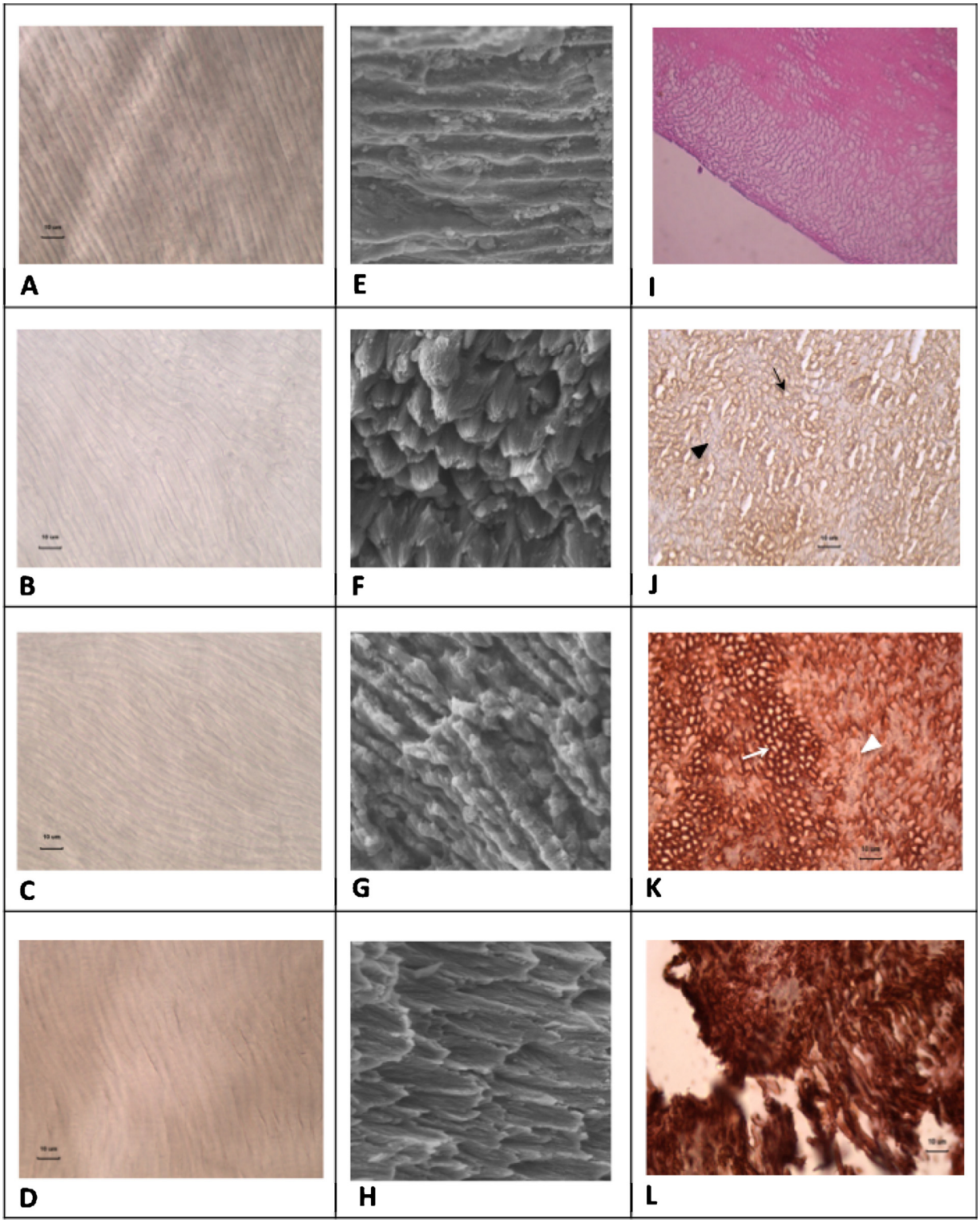

Fig. 2 – Images A–D: histological, E–H: ultrastructural, I: histopathological and J–L: immunohistochemical analysis of the enamel of teeth affected with hypocalcified AI. Enamel ground sections of the deciduous second molar of proband FAI2-III.5 (A), the third molar of proband FAI5-II.1 (B), the third molar of proband FAI14-II.1 (C) and the third molar of a normal subject (D). Photographs of SEM of the enamel from deciduous second molar of proband FAI2-II.1 (E), the third molar of proband FAI5-II.1 (F), the third molar of proband FAI14-II.1 (G) and the third molar of a normal subject (H). Haematoxylin and Eosin staining of the enamel from deciduous second molar of proband FAI2-III.5, showing enamel that retains a lots of organic matter (I). Photomicrographs of the immunohistochemical technique using the anti-amelogenin antibody in enamel of the third molar of proband FAI5-II.1 (J), the third molar of proband FAI14-II.1 (K) and a included third molar as positive control (L).

in the sample from proband II.1 of family FAI5 (Fig. 2J) and through red staining in proband II.1 of family FAI14 (Fig. 2K). Moreover, in both preparations, areas of prismatic enamel (Fig. 2J, black arrow and Fig. 2K, white arrow) and amorphous areas of aprismatic enamel (Fig. 2J, black arrowhead and Fig. 2K, white arrowhead) could be observed. With respect to the areas of prismatic enamel, brown staining was found in both the periphery and interior of the prisms in the sample from the proband II.1 of family FAI5 (Fig. 2J, black arrow), whereas the reddish staining was confined to the periphery of the prisms in the sample from proband II.1 of family FAI14 (Fig. 2K, white arrow). Unfortunately, due to the exhaustion of the study material, this technique could not be performed in the sample from proband III.5 of family FAI2, however the histopathological analysis using H&E staining, showed persistence of organic matter in the affected enamel (Fig. 2I).

Moreover, the study of the negative controls for the teeth of probands II.1 of family FAI14 and II.1 of family FAI5 using phosphate-buffered saline instead of the anti-amelogenin antibody showed no staining (not shown), whereas the analysis of the positive controls resulted in intense labelling. In the case of the advanced bell stage tooth germ, intense brownish staining that was relatively abundant compared with the matrix secreted by the ameloblasts was observed (not shown); in the case of the third molar, intense reddish staining was observed in the sample (Fig. 2L).

4. Discussion

This study characterized patients with AI from three unrelated Chilean families from clinical, radiographic, histological, immunohistochemical and genetic perspectives. As the *FAM83H* gene is the only gene to date in which causal mutations have been linked to hypocalcified AI, it was decided to molecularly analyze this gene in the recruited probands. Also teeth had been voluntarily donated by the probands and their parents, which allowed for a macro and ultrastructural study, using light microscopy and SEM. Moreover, in two of the cases studied (II.1 FAI5 and II.1 FAI14), the presence or absence of amelogenin-like proteins was determined by immunohistochemistry on tooth sections.

4.1. *Clinical and radiographic analysis*

The clinical features of three patients are most consistent with hypocalcified AI (Fig. 1A–C), exhibiting characteristics similar to those proposed in the classification by Witkop[4] and described in other studies with the same type of AI, such as the following: yellowish-brown staining, rough texture, wear or loss of enamel upon eruption and a similar contrast between the dentine and enamel.[7,34,35,42,43]

Although AI corresponds to an alteration in the structure and appearance of the enamel, other dental anomalies may coexist,[57] such as the delayed eruption in proband III.5 of the FAI2 family. In addition, the three probands were diagnosed with generalized gingivitis, which was most likely due to the rough surface of the enamel that allowed for the retention of plaque, which adds dental hypersensitivity to thermal stimuli hindering proper oral hygiene. Additionally, the three affected individuals had composite restorations that were fractured or failed after a period of time, which may be due to poor adherence of the material to the affected enamel surface. Notably, proband II.1 of the FAI14 family (Fig. 1C) showed some particular clinical features, such as average enamel thickness in the middle region and less intense discolouring of the enamel in the cervical region. Some of their teeth, especially the lower molars, were relatively intact, enabling their crown anatomy to be distinguished on radiographs with a slightly higher contrast in the enamel. Other studies[7,37] have also described distinctive phenotypes in some families affected with hypocalcified AI, with the diagnoses confirmed by the finding of mutations in the *FAM83H* gene. Wright et al.[37] found that affected individuals in two families had hypocalcified enamel exclusively in the cervical third of the teeth. Song et al.[7] found that the affected members of a family had the classic features of hypocalcified enamel but a polished and shiny surface. These observations confirm the great clinical and radiographic variability that may exist not only between different types of AI but also within the same clinical type.

4.2. *Genetic and molecular analysis*

The pedigree of family FAI2 revealed that subject III.5 was the only one affected (Fig. 1A). While individual IV.2 was reported to be affected, he was not examined, suggesting recessive inheritance or sporadic-case in all three families. The pedigrees comprise only two generations, and thus an inheritance pattern cannot be established with certainty (Fig. 1B and C) nor can sporadic cases corresponding to spontaneous or de novo mutations be confirmed.

The mutational analysis of gene *FAM83H* involved the study of the entire coding sequence and intron–exon neighbourhoods using PCR and direct sequencing. No mutation in this gene was found in the DNA from two probands; FAI2-II.5 and FAI5-II.1. However, in proband II.1 of family FAI14, the variant g.10953G>T (c.1669G>T; p.Gly557Cys) was found (Fig. 1C), which has not been reported as a SNP or as a previously described causal mutation when it was discovered. Co-segregation analysis by direct sequencing using DNA from the mother, half-sister and 15 healthy controls without AI revealed that none of the relatives or controls had that variant. Furthermore, a PCR-RFLP analysis designed in the laboratory for the presence of variant g.10953G>T was performed in 100 healthy controls, including 15 subjects previously verified by direct sequencing. These results and the absence of the variant in the SNP database and the 1000 genomes project support the finding that this sequence change is the cause of the clinical phenotype in the FA14 family.

The paralogous sequence alignment of eight family members of the FAM83 family (FAM83 A-H) with orthologous sequences in seven vertebrate species performed by Ding et al.[39] showed that G^{557} corresponds to a relatively conserved amino acid; four members of the FAM83 family and three species of mammals, which are closer on the evolutionary scale (human, mouse and bovine), had a conserved glycine in the aforementioned position. The *missense* change of p.Gly557Cys likely affects the function of the gene product as cysteine is able to form disulfide bonds, which may alter the three-dimensional structure of the protein and thereby affect

its function. The *in silico* prediction of bond formation with metals and formation of disulfide bridges showed that C^{557} did not produce metal bonds but did alter the pattern of disulfide bonds within the mutant protein compared with the wild-type because the latter may generate disulfide bonds with C^{590} and C^{1090} whereas the mutant can form bonds with C^{557}, C^{590} or C^{1090}. The PolyPhen 2.0, PANTHER and PMut programmes showed that the p.Gly557Cys substitution is most likely pathogenic with scores of 0.992, 0.851 and 0.841, respectively.

All alterations reported to date in the *FAM83H* gene correspond to nonsense and frameshift mutations (Table 2) that introduce a premature stop codon between amino acids S^{287} and E^{694}, resulting in a truncated protein.[7,36,37,43] These truncated proteins will interfere with the normal protein and produce the phenotype through a dominant negative effect on the wild-type protein.[40] Although the mutation reported in this study (g.10953C>T, c.1669G>T and p.Gly557Cys) is located in the same region of exon 5 of *FAM83H* where all known mutations have been reported, this report is the first of a *missense* mutation causing an amino acid change in the protein that is associated with a phenotype of generalized enamel, although the phenotype is attenuated or less severe than those described above (Table 2).

At present, at what stage of the process of amelogenesis does the defect that causes hypocalcified AI occurs is unknown; if this occurs in the primary mineralization during the secretory stage, or if this happens in the secondary mineralization during the maturation stage, or another instance between or throughout the two stages.

Until recently, the role of *FAM83H* was largely unknown. Ding et al.[39] reported that mouse Fam83h is located in the intracellular environment and is associated with perinuclear vesicles in the vicinity of the Golgi apparatus. Subsequently, Lee et al.[36] demonstrated *in vitro* that the mutations p.Q677*, p.W460* and p.R325* altered the localization of the protein, increasing its concentration within the nucleus.

Recent reports attributed FAM83H a role in the development of various cancers.[58–60] The study by Kuga et al.[61] conducted on cell lines and tumour tissues of colorectal cancer demonstrated in vitro and in vivo that FAM83H associates with casein kinase 1 alpha (CK-1α) and with keratins 8 and 18. In this association, FAM83H participates as a linker protein

Table 2 – Reported mutations to date in exon 5 of the *FAM83H* gene.

No.	cDNA	Protein	Family ID	Ethnicity	Pattern of inheritance	References	Clinical phenotype
1	c.973C>T	p.R325*	F1ADHCAI	Korean	AD	Kim JW, 2008[34]	Generalized hypocalcified
			Family 3	Chinese	AD	Song YL, 2012[7]	
2	c.1192C>T	p.Q398*	F2ADHCAI	Korean	Sporadic	Kim JW, 2008[34]	Generalized hypocalcified
			Family 1	Turkish	AD	Hart PS, 2009[40]	
			Family 2	Caucasian	AD	Ding Y, 2009[39]	
			No ID	No data	No data	Wright JT, 2011[38]	No described
3	c.1243G>T	p.E415*	F1(AI#8)	Hispanic	AD	Lee SK, 2008[35]	Generalized hypocalcified
4	c.891T>A	p.Y297*	F2(AI#12)	Asian	Sporadic	Lee SK, 2008[35]	Generalized hypocalcified
5	c.1380G>A	p.W460*	F3(AI#21)	Caucasian	AD	Lee SK, 2008[35]	Generalized hypocalcified
6	c.2029C>T	p.Q677*	F4(AI#24)	Caucasian	AD	Lee SK, 2008[35]	Generalized hypocalcified
			Family 38	Caucasian	AD	Chan HC, 2011[10]	
			Family 2,III.2	Korean	AD	Lee SK, 2011[36]	
			Family 5, III.3	Chinese	AD	Song YL, 2012[7]	
			No ID	No data	No data	Wright JT, 2011[38]	No described
7	c.1330C>T	p.Q444*	F2, III.1	Turkish	AD	Hart PS, 2009[40]	Generalized hypocalcified
			Family 1, II.3	Hispanic	AD	Ding Y, 2009[39]	
8	c.1366C>T	p.Q456*	F3-F8	Turkish	5 AD, 1 Sproradic	Hart PS, 2009[40]	Generalized hypocalcified
9	c.1408C>T	p.Q470*	AIC5, AIC33	Caucasian	AD	Wright JT, 2009[37]	Generalized hypocalcified
10	c.860C>A	p.S287*	AIC19	Caucasian	AD	Wright JT, 2009[37]	Generalized hypocalcified
11	c.923_924delTC	p.L308fs*323	AIC38	Caucasian	AD	Wright JT, 2009[37]	Generalized hypocalcified
12	c.1379G>A	p.W460*	AIC40	Caucasian	AD	Wright JT, 2009[37]	Generalized hypocalcified
13	c.1872_1873delCC	p.L625fs*703	AIC46	Caucasian	AD	Wright JT, 2009[37]	Localized hypocalcified
14	c.2080G>T	pE694*	AI10-002	Caucasian	Sporadic	Wright JT, 2009[37]	Localized hypocalcified
15	c.1354C>T	p.Q452*	F1,III.3	Korean	AD	Hyun HK, 2009[41]	Generalized hypocalcified
			Family 39	Caucasian	AD	Chan HC, 2011[10]	
			Family 4, III.4	Chinese	AD	Song YL, 2012[7]	
			Family 2	Danish	AD	Haubek D, 2011[43]	
16	c.1993C>T	p.Q665*	Fam1, III.1	Korean	AD	Lee SK, 2011[36]	Generalized Hipoplast/ hypomin
17	c.1374C>A	p.Y458*	Fam1, V.1	European	AD	El-Sayed W, 2010[42]	Generalized hypocalcified
18	c.906T>G	p.Y302*	Fam 1, IV.12	Danish	AD	Haubek D, 2011[43]	Generalized hypocalcified
			Family 2, III.1	Chinese	AD	Song YL, 2012[7]	
19	c.1289C>A	p.S430*	No ID	No data	No data	Wright JT, 2011[38]	No described
20	c.924dupT	p.V309Rfs*324	Fam 1, IV.14,	Chinese	AD	Song YL, 2012[7]	Generalized hypocalcified
21	c.1669G>T	p.G557C	FAI14LP	Chilean	Sporadic	This study	Generalized hypocalcified, attenuated

between CK-1α and keratins. FAM83H interacts with CK-1α by means of its amino terminal region and the amino acid sequence FDEEFRILF and its carboxyl terminus binds keratins. Thus, FAM83H can recruit CK-1α to keratin filaments, enabling CK-1α to modulate the filamentous status of keratins by phosphorylation/dephosphorylation. Under normal conditions, the levels of FAM83H expression orchestrate the subcellular distribution and function of CK-1α, thereby allowing FAM83H to regulate the keratin cytoskeleton organization by recruiting CK-1α to the filaments.[61] These observations allow us to suggest that the g.10953C>T mutation, acting via a mechanism of haploinsufficiency, could disrupt the cytoskeletal keratins and partially affect the function of the ameloblasts and enamel synthesis, thus explaining the more attenuated clinical phenotype observed in the proband. Moreover, the phenotype associated with the same case, i.e., the retention of amelogenin in the periphery of the prisms, which was observed in the tooth of the proband, could be explained by the simultaneous gain of a regulatory function of *FAM83H* on the expression and/or degradation of amelogenin during amelogenesis.

In patient III.5 of the FAI2 family and patient II.1 of the FAI5 family, no mutations in *FAM83H* explain their phenotype, similar to the findings in other studies on hypocalcified AI. For example, Lee et al.[35] found mutations in only four of seven families; three had AD inheritance and the other had a de novo mutation. Haubek et al.[43] found mutations in two of six families, one with AD inheritance and the other with a *de novo* mutation. Finally, Song et al.[7] found causal mutations in five of six families, with all showing AD inheritance. From our study, we cannot rule out the existence of causal mutations in non-coding or regulatory regions of the *FAM83H* gene that were not analyzed in this study or previous studies or the presence of other yet to be discovered enamel genes that may also be responsible for AI in families where causal mutations have not been determined.

4.3. *Histological, ultrastructural and immunohistochemical analyses*

Previous studies in hypocalcified AI teeth using light microscopy and SEM reported diverse results. Some studies have described areas of prismatic enamel with non-crystalline amorphous material, possibly proteins; crystals with a normal shape, size and orientation but of higher porosity and that are more labile[37]; prismatic structure with cracks or crevices that could not have any mineral content[41]; incomplete malformed prisms with presence of amorphous material, which may indicate organic material retention.[42] Similarly, in this study, diverse results were also found. The light microscopy and SEM analyses showed that the enamel prismatic structure of the teeth of proband III.5 of FAI2 family and proband II.1 of family FAI5 appeared similar to that observed in the controls. However, in the tooth of proband II.1 of family FAI14, the prism structure did not maintain a constant diameter under SEM, with upraised projections, and some sectors that maintain irregular prismatic structure.

The immunohistochemical analysis detected the presence of amelogenin, demonstrated by an intense brown labelling, both inside and on the periphery of the enamel prism of the tooth of the proband II.1 of family FAI5. In the sample from proband II.1 of family FAI14, bright red labelling was observed only in the periphery of the prisms, suggesting that in the latter case, the organic component of the interior of the prisms is removed in a timely manner. Unfortunately, which of the two samples had less remaining amelogenin could not be determined, which would have been interesting because if proband II.1 of family FAI14 had less, the phenotype could be relate to his crown anatomy more conserved and the largest contrast between the enamel and dentine in some of his teeth. Other studies using the teeth of subjects affected with hypocalcified AI have also found a high protein content[37,62,63] and in some cases, reactivity has been demonstrated with anti-amelogenin antibody by western blot analysis.[63,64] Because the average protein content of mature enamel is less than 1%, the higher protein content, combined with a lower mineral content, is postulated to cause the enamel to wear easily and serve as a poor insulator against thermal changes, causing hypersensitivity.[37]

5. Conclusions

These results suggest that *FAM83H missense* mutation reported in one of the families analyzed in this study might cause a phenotype of hypocalcified enamel more attenuated with retention of amelogenin. Additional experimental studies and new approaches to elucidate the effects of this mutation on the clinical phenotype of the enamel and to further define the mechanisms that simultaneously affect tissue formation and degradation as well as amelogenin expression during the formation thereof are required.

Authors' contributions

B.U. conceived the study and its design, recruited and interviewed patients, coordinated, designed, conducted various experiments and supervised all molecular genetic study, drafted and wrote the manuscript, leads the research project and funding. C.M. participated in part of molecular genetic and part of clinical and histological analysis. A.O.P. participated in clinical examination and assessment of patients, interpretation of histological results, and contributed in writing and revising the manuscript. D.A. performed clinical examination and assessment of patients. A.P. helped with the molecular studies. I.M.B., L.J., C.L. and C.L. participated in data analysis and critical review of the manuscript. G.R. performed the bioinformatic analysis. M.R. performed the histological and inmunohistochemical analysis.

Funding

This research was funded by Projects Fondecyt No. 1140905, FIOUCh 13-001 and PRI-ODO 12/008.

Competing interests

The authors declare that they have no competing interests.

Ethical approval

This project was approved by Scientific Ethical Committee, Faculty of Dentistry of the University of Chile (CEC-FOUCH). Informed consent/assent was obtained from all participants and their parents.

Acknowledgements

The authors thank Professor Jan Ching Chun Hu of the University of Michigan for her review of this manuscript and comments. The authors thank the participating families for their cooperation.

REFERENCES

1. Simmer JP, Fincham AG. Molecular mechanisms of dental enamel formation. *Crit Rev Oral Biol Med* 1995;**6**:84–108.
2. Simmer JP, Richardson AS, Hu YY, Smith CE, Ching-Chun Hu J. A post-classical theory of enamel biomineralization... and why we need one. *Int J Oral Sci* 2012;**4**:129–34.
3. Moradian-Oldak J. Protein-mediated enamel mineralization. *Front Biosci* 2012;**17**:1996–2023.
4. Witkop CJ. Amelogenesis imperfecta dentinogenesis imperfecta and dentin dysplasia revisited: problems in classification. *J Oral Pathol* 1989;**17**:547–53.
5. Crawford PJ, Aldred M, Bloch-Zupan A. Amelogenesis imperfecta. *Orphanet J Rare Dis* 2007;**4**:2–17.
6. Aldred MJ, Savarirayan R, Crawford PJ. Amelogenesis imperfecta: a classification and catalogue for the 21st century. *Oral Dis* 2003;**9**:19–23.
7. Song YL, Wang CN, Zhang CZ, Yang K, Bian Z. Molecular characterization of amelogenesis imperfecta in Chinese patients. *Cells Tissues Organs* 2012;**196**:271–9.
8. El-Sayed W, Parry DA, Shore RC, Ahmed M, Jafri H, Rashid Y, et al. Mutations in the beta propeller *WDR72* cause autosomal-recessive hypomaturation amelogenesis imperfecta. *Am J Hum Genet* 2009;**85**:699–705.
9. El-Sayed W, Shore RC, Parry DA, Inglehearn CF, Mighell AJ. Hypomaturation amelogenesis imperfecta due to *WDR72* mutations: a novel mutation and ultrastructural analyses of deciduous teeth. *Cells Tissues Organs* 2011;**194**:60–6.
10. Chan HC, Estrella NM, Milkovich RN, Kim JW, Simmer JP, Hu JC. Target gene analyses of 39 amelogenesis imperfecta kindreds. *Eur J Oral Sci* 2011;**119**(Suppl. 1):311–23.
11. Sundell S, Valentin J. Hereditary aspects and classification of hereditary amelogenesis imperfecta. *Community Dent Oral Epidemiol* 1986;**14**:211–6.
12. Chosack A, Eidelman E, Wisotski I, Cohen T. Amelogenesis imperfecta among Israeli Jews and the description of a new type of local hypoplastic autosomal recessive amelogenesis imperfecta. *Oral Surg Oral Med Oral Pathol* 1979;**47**:148–56.
13. Witkop CJ. Hereditary defects in enamel and dentin. *Acta Genet Stat Med* 1957;**7**:236–9.
14. Wright JT, Hart PS, Aldred MJ, Seow K, Crawford PJ, Hong SP, et al. Relationship of phenotype and genotype in X-linked amelogenesis imperfecta. *Connect Tissue Res* 2003;**44**(Suppl. 1):72–8.
15. Lee KE, Lee SK, Jung SE, Song SJ, Cho SH, Lee ZH, et al. A novel mutation in the *AMELX* gene and multiple crown resorptions. *Eur J Oral Sci* 2011;**119**(Suppl. 1):324–8.
16. Hu JC, Chan HC, Simmer SG, Seymen F, Richardson AS, Hu Y, et al. Amelogenesis imperfecta in two families with defined AMELX deletions in ARHGAP6. *PLoS ONE* 2012;**7**:e52052.
17. Simmer SG, Estrella NM, Milkovich RN, Hu JC. Autosomal dominant amelogenesis imperfecta associated with *ENAM* frameshift mutation p.Asn36Ilefs56. *Clin Genet* 2013;**83**:195–7.
18. Poulter JA, El-Sayed W, Shore RC, Kirkham J, Inglehearn CF, Mighell AJ. Whole-exome sequencing, without prior linkage, identifies a mutation in *LAMB3* as a cause of dominant hypoplastic amelogenesis imperfecta. *Eur J Hum Genet* 2013;**22**:132–5.
19. Kim JW, Seymen F, Lee KE, Ko J, Yildirim M, Tuna EB, et al. *LAMB3* mutations causing autosomal-dominant amelogenesis imperfecta. *J Dent Res* 2013;**92**:899–904.
20. Lee KE, Ko J, Tran Le CG, Shin TJ, Hyun HK, Lee SH, et al. Novel *LAMB3* mutations cause non-syndromic amelogenesis imperfecta with variable expressivity. *Clin Genet* 2015;**87**(1):90–2.
21. Hart TC, Hart PS, Gorry MC, Michalec MD, Ryu OH, Uygur C, et al. Novel ENAM mutation responsible for autosomal recessive amelogenesis imperfecta and localised enamel defects. *J Med Genet* 2003;**40**:900–6.
22. Ozdemir D, Hart PS, Firatli E, Aren G, Ryu OH, Hart TC. Phenotype of ENAM mutations is dosage-dependent. *J Dent Res* 2005;**84**:1036–41.
23. Parry DA, Brookes SJ, Logan CV, Poulter JA, El-Sayed W, Al-Bahlani S, et al. Mutations in *C4orf26*, encoding a peptide with in vitro hydroxyapatite crystal nucleation and growth activity, cause amelogenesis imperfecta. *Am J Hum Genet* 2012;**91**:565–71.
24. Poulter JA, Brookes SJ, Shore RC, Smith CE, Abi Farraj L, Kirkham J, et al. A *missense* mutation in ITGB6 causes pitted hypomineralized amelogenesis imperfecta. *Hum Mol Genet* 2014;**23**(8):2189–97.
25. Wang SK, Choi M, Richardson AS, Reid BM, Lin BP, Wang SJ, et al. ITGB6 loss-of-function mutations cause autosomal recessive amelogenesis imperfecta. *Hum Mol Genet* 2014;**23**(8):2157–63.
26. Poulter JA, Murillo G, Brookes SJ, Smith CE, Parry DA, Silva S, et al. Deletion of ameloblastin exon 6 is associated with amelogenesis imperfecta. *Hum Mol Genet* 2014;**23**:5317–24.
27. Wang SK, Hu Y, Simmer JP, Seymen F, Estrella NM, Pal S, et al. Novel *KLK4* and *MMP20* mutations discovered by whole-exome sequencing. *J Dent Res* 2013;**92**:266–71.
28. Gasse B, Karayigit E, Mathieu E, Jung S, Garret A, Huckert M, et al. Homozygous and compound heterozygous *MMP20* mutations in amelogenesis imperfecta. *J Dent Res* 2013;**92**:598–603.
29. Hart PS, Hart TC, Michalec MD, Ryu OH, Simmons D, Hong S, et al. Mutation in kallikrein 4 causes autosomal recessive hypomaturation amelogenesis imperfecta. *J Med Genet* 2004;**41**:545–9.
30. Kuechler A, Hentschel J, Kurth I, Stephan B, Prott EC, Schweiger B, et al. A novel homozygous *WDR72* mutation in two siblings with amelogenesis imperfecta and mild short stature. *Mol Syndromol* 2012;**3**:223–9.
31. Parry DA, Poulter JA, Logan CV, Brookes SJ, Jafri H, Ferguson CH, et al. Identification of mutations in *SLC24A4*, encoding a potassium-dependent sodium/calcium exchanger, as a cause of amelogenesis imperfecta. *Am J Hum Genet* 2013;**92**:307–12.
32. Seymen F, Lee KE, Tran Le CG, Yildirim M, Gencay K, Lee ZH, et al. Exonal deletion of *SLC24A4* causes hypomaturation amelogenesis imperfecta. *J Dent Res* 2014;**93**(4):366–70.
33. Wang S, Choi M, Richardson AS, Reid BM, Seymen F, Yildirim M, et al. *STIM1* and *SLC24A4* are critical for enamel maturation. *J Dent Res* 2014;**93**:94S–100S.
34. Kim JW, Lee SK, Lee ZH, Park JC, Lee KE, Lee MH, et al. *FAM83H* mutations in families with autosomal-dominant

hypocalcified amelogenesis imperfecta. *Am J Hum Genet* 2008;**82**:489–94.
35. Lee SK, Hu JC, Bartlett JD, Lee KE, Lin BP, Simmer JP, et al. Mutational spectrum of *FAM83H*: the C-terminal portion is required for tooth enamel calcification. *Hum Mutat* 2008;**29**:E95–9.
36. Lee SK, Lee KE, Jeong TS, Hwang YH, Kim S, Hu JC, et al. *FAM83H* mutations cause ADHCAI and alter intracellular protein localization. *J Dent Res* 2011;**90**:377–81.
37. Wright JT, Frazier-Bowers S, Simmons D, Alexander K, Crawford P, Han ST, et al. Phenotypic variation in *FAM83H*-associated amelogenesis imperfecta. *J Dent Res* 2009;**88**:356–60.
38. Wright JT, Torain M, Long K, Seow K, Crawford P, Aldred MJ, et al. Amelogenesis imperfecta: genotype–phenotype studies in 71 families. *Cells Tissues Organs* 2011;**194**:279–83.
39. Ding Y, Estrella MR, Hu YY, Chan HL, Zhang HD, Kim JW, et al. Fam83h is associated with intracellular vesicles and ADHCAI. *J Dent Res* 2009;**88**:991–6.
40. Hart PS, Becerik S, Cogulu D, Emingil G, Ozdemir-Ozenen D, Han ST, et al. Novel *FAM83H* mutations in Turkish families with autosomal dominant hypocalcified amelogenesis imperfecta. *Clin Genet* 2009;**75**:401–4.
41. Hyun HK, Lee SK, Lee KE, Kang HY, Kim EJ, Choung PH, et al. Identification of a novel FAM83H mutation and microhardness of an affected molar in autosomal dominant hypocalcified amelogenesis imperfecta. *Int Endod J* 2009;**42**:1039–43.
42. El-Sayed W, Shore RC, Parry DA, Inglehearn CF, Mighell AJ. Ultrastructural analyses of deciduous teeth affected by hypocalcified amelogenesis imperfecta from a family with a novel Y458X *FAM83H* nonsense mutation. *Cells Tissues Organs* 2010;**191**:235–9.
43. Haubek D, Gjørup H, Jensen LG, Juncker I, Nyegaard M, Børglum AD, et al. Limited phenotypic variation of hypocalcified amelogenesis imperfecta in a Danish five-generation family with a novel *FAM83H* nonsense mutation. *Int J Paediatr Dent* 2011;**21**:407–12.
44. Kweon YS, Lee KE, Ko J, Hu JC, Simmer JP, Kim JW. Effects of Fam83h overexpression on enamel and dentine formation. *Arch Oral Biol* 2013;**58**:1148–54.
45. WMA Declaration of Helsinki-Ethical Principles for Medical Research Involving Human Subjects. *64th WMA General Assembly, Fortaleza, Brazil*. October 2013. http://www.wma.net/es/30publications/10policies/b3/.
46. Miller SA, Dykes DD, Polesky HF. A simple salting out procedure for extracting DNA from human nucleated cells. *Nucleic Acids Res* 1988;**16**:1215.
47. Primer-BLAST software. http://www.ncbi.nlm.nih.gov/tools/primer-blast/.
48. PolyPhen v 2.0 software. http://genetics.bwh.harvard.edu/pph2/.
49. Protein ANnotation THrough Evolutionary Relationship software (PANTHER). http://www.pantherdb.org/.
50. Pathological Mutations software (PMut). http://mmb2.pcb.ub.es:8080/PMut/.
51. Server DiAminoacid Neural Network Application software (DiANNA). http://clavius.bc.edu/~clotelab/DiANNA/.
52. Database of Interacting Proteins software (DIP). http://dip.doe-mbi.ucla.edu/dip/Main.cgi/.
53. Database of Human Protein-Protein Interaction Prediction software (PIPs). http://www.compbio.dundee.ac.uk/www-pips/.
54. SNP database. http://www.ncbi.nlm.nih.gov/snp/.
55. Urzúa B, Ortega-Pinto A, Farias DA, Franco E, Morales-Bozo I, Moncada G, et al. A multidisciplinary approach for the diagnosis of hypocalcified amelogenesis imperfecta in two Chilean families. *Acta Odontol Scand* 2012;**70**:7–14.
56. 1000 genomes Project. A deep catalog of Human Genetic Variation. http://www.1000genomes.org/home.
57. Hunter L, Addy LD, Knox J, Drage N. Is amelogenesis imperfecta an indication for renal examination? *Int J Paediatr Dent* 2007;**17**:62–5.
58. Hatanaka H, Takada S, Tsukui M, Choi YL, Kurashina K, Soda M, et al. Identification of the transforming activity of Indian hedgehog by retroviral expression screening. *Cancer Sci* 2010;**101**:60–4.
59. Sasaroli D, Gimotty PA, Pathak HB, Hammond R, Kougioumtzidou E, Katsaros D, et al. Novel surface targets and serum biomarkers from the ovarian cancer vasculature. *Cancer Biol Ther* 2011;**12**:169–80.
60. Klammer M, Kaminski M, Zedler A, Oppermann F, Blencke S, Marx S, et al. Phosphosignature predicts dasatinib response in non-small cell lung cancer. *Mol Cell Proteomics* 2012;**11**:651–68.
61. Kuga T, Kume H, Kawasaki N, Sato M, Adachi J, Shiromizu T, et al. A novel mechanism of keratin cytoskeleton organization through casein kinase Iα and FAM83H in colorectal cancer. *J Cell Sci* 2013;**126**:4721–31.
62. Wright JT, Deaton TG, Hall KI, Yamauchi M. The mineral and protein content of enamel in amelogenesis imperfecta. *Connect Tissue Res* 1995;**32**:247–52.
63. Wright JT, Hall KI, Yamauche M. The enamel proteins in human amelogenesis imperfecta. *Arch Oral Biol* 1997;**42**:149–59.
64. Takagi Y, Fujita H, Katano H, Shimokawa H, Kuroda T. Immunochemical and biochemical characteristics of enamel proteins in hypocalcified amelogenesis imperfecta. *Oral Surg Oral Med Oral Pathol Oral Radiol Endod* 1998;**85**:424–30.